AIAA JOURNAL
Vol. 47, No. 12, December 2009

Technical Notes

Flow Visualization Study of the Aerodynamics of Modeled Dragonfly Wings

A. Obata* and S. Sinohara†
Nippon Bunri University, Oita 870-0397, Japan

DOI: 10.2514/1.43836

Introduction

ALTHOUGH our knowledge of steady flows around the wings of dragonflies at Reynolds numbers Re on the order of 10^3 is very limited (Re is defined here based on the wing chord length and the uniform flow velocity), it is known that dragonfly wings exhibit the aerodynamic feature of forming vortices around them [1–5]. As pointed out by Ellington [6], however, the mechanisms responsible for the excellent aerodynamic and flight dynamic characteristics recognized in the gliding dragonfly have hitherto remained unsolved.

Even though results of precise particle image velocimetry observation of vortices generated by modeled dragonfly wings are presented by Tamai et al. [7], only localized features close to the upper surface of the wings were revealed, and no observations or descriptions were extended to the role of vortices in the flow around the wings.

The purpose of the present study is to visualize flows around the corrugated wings of dragonflies, using two improved visualization methods and two-dimensional model wings placed in a circulatory, open-type water tank, and thereby to investigate the aerodynamic mechanisms by which dragonfly wings exhibit such a distinct ability in low-Re flows.

Flow Visualization Methods

A circulatory, open-type, acrylic resin water tank of external dimensions 6×3 m and width 75 cm, incorporating a test section of length 190 cm, was constructed to visualize flows around modeled corrugated wings of dragonflies. The test section of the tank and a surface flow pattern viewed slightly obliquely from the top are shown in Figs. 1a and 1b, respectively. The flow velocity favorable for flow visualization ranged from 1.0 to 5.0 cm/s; these velocities were measured with a thermal flow meter calibrated with a laser Doppler velocimeter.

The measurement apparatus in the test section consists of twin rails on the bottom, a flat base plate supported by twin vertical plates sliding on the rails, a vertically installed two-dimensional wing model on the base plate, connected push–pull plates, and a straddling dolly. The base plate was 1.5 cm thick, 90 cm long, and 60 cm wide; it was positioned at a height of half the depth of the tank.

A thin turntable was embedded in the base plate with a thin narrow-shaped groove into which a two-dimensional wing model with the groove-shaped thin plate at the root could be installed. The two-dimensional wing model, with a chord length of about 20 cm, was fixed to the groove-shaped bottom plate that was smoothly fitted into the turntable and projected 16 cm vertically into the test section. A tall dolly straddling the test section of the water tank was also installed so as to help carry out the experiments.

Stepwise acceleration of the wing in a steady flow is made possible by accelerating the dolly stepwise. The dolly pushes the thin flat plates such that the connected wing model moves forward in the uniform flowfield. The dolly moves parallel to the tank on a ground-mounted rail, and exhibits adequate response and accuracy for speeds less than 5 cm/s due to the servomotor control system.

In the current study, an improvement of the aluminum tracer method (Karman [8]) facilitated flow visualization. The aluminum tracer method was improved by forming a linear region containing no aluminum particles parallel with the flow along the surface to be observed. To enhance the visibility of the flow, an array of light-emitting diodes was used. Provided the exposure time for observational photography is properly selected, this method displays the mean streamlines of the entire flowfield and the mean movements of wakes and vortices, enabling an average relationship between the lift-to-drag characteristics of wings and the vortices around them to be established.

It is apparent that a larger curvature of the streamlines around the wing will cause a larger lift or down force acting on the wing, because the centrifugal forces on flow particles are transmitted to the wing surfaces. Analysis of the flow pattern in the wake or separated region also enables us to comprehend the drag characteristics of the wing. The presence of stagnant flow in the separated region allows us to conclude that the drag of this wing at low Re is far greater than that at higher Re where the flow is free from separation.

The flow visualization method of observing the emanation of a painted tracer (Taneda [9]) at a resolving level of visualization,

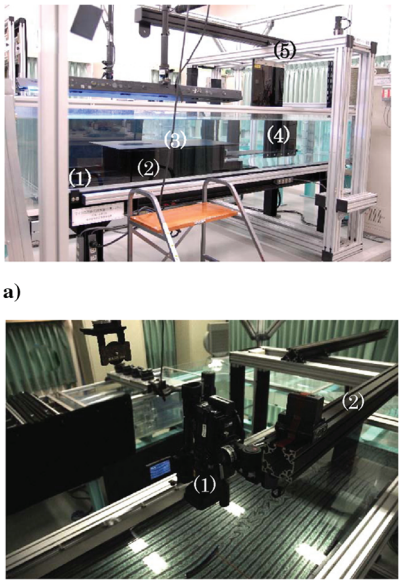

Fig. 1 Side and overhead view of the test-section of circulatory water tank: a) overall features of test section of water tank, showing (1) twin rails, (2) sliding twin vertical plates, (3) base plate, (4) push–pull plates, and (5) straddling dolly; b) overhead view of two-dimensional flow patterns around a curved plate with (1) the video camera and (2) its supporting beam, extended from the dolly.

Received 15 February 2009; revision received 9 June 2009; accepted for publication 14 June 2009.

*Professor, Department of Aerospace Engineering, and Micro Flying Robot Laboratory, Itigi 1727; obata@nbu.ac.jp (Corresponding Author).
†Graduate Student, Engineering Graduate Course, Itigi 1727.

a)

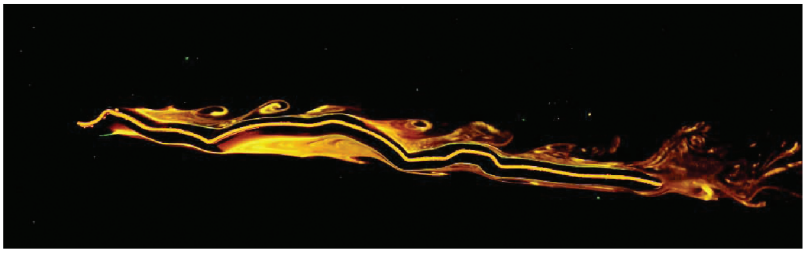

b)

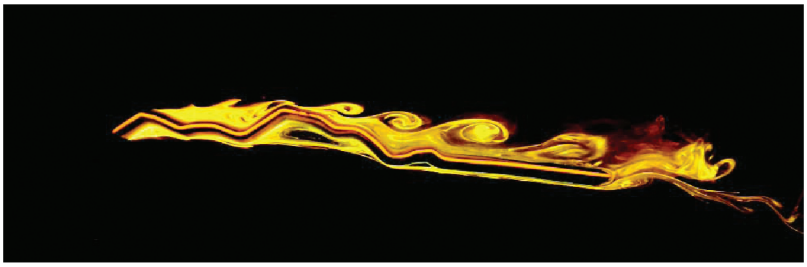

c)

d)

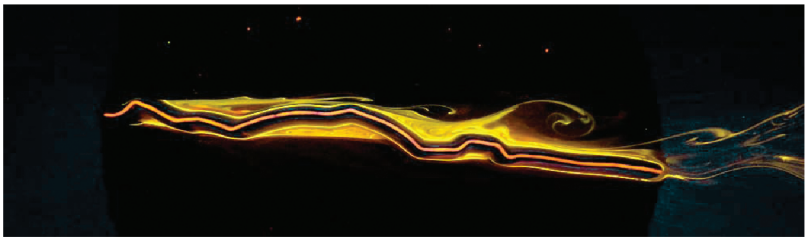

e)

f)

Fig. 2 Flows around wing models of the dragonfly *Anax parthenope* (cross section at the 75% semispan location) at an angle of attack of 5 deg: a) flow around a hindwing section at $Re \approx 7000$; b) vortex train around a hindwing section at $Re = 7000$; c) vortex train around a forewing model at the same sectional position as the hindwing at $Re \approx 7000$; d) flow around a forewing model at the same sectional position as 2c at $Re \approx 7000$; e) vortex train around a hindwing model at $Re \approx 3500$; f) flow around a hindwing section at $Re \approx 2000$.

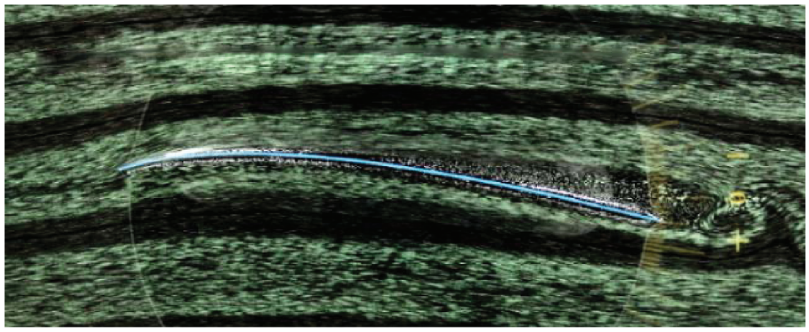

a) Cambered airfoil before acceleration (Benedek 6%)

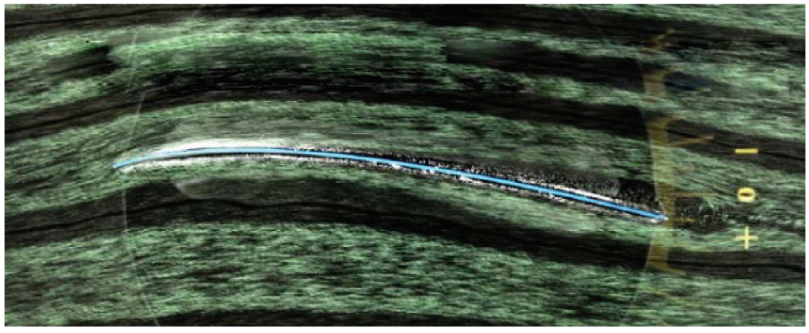

b) Cambered airfoil after acceleration and a relative forward displacement of 1.8 chord lengths

c) *Anax parthenope*'s hindwing before acceleration

d) *Anax parthenope*'s hindwing after acceleration and a relative forward displacement of 1.8 chord lengths

Fig. 3 Change of flows around wing sections before and after acceleration.

enhanced by the use of laser sheet lights together with ultraviolet light, is suitable for observing vortices (Honji [10]) and serves to complement the interpretation of the experimental results based on the aluminum tracer method, because we can observe how the vortices are generated and deformed above and below the wings. Consequently, four laser sheet lights were used to illuminate the flow around the model from both sides of the tank through the acrylic resin plate wall.

Conclusions

We selected the dragonfly *Anax parthenope*, known as the lesser emperor, for which the dimensions of its wing cross sections have been described in detail (Okamoto et al. [1]), and conducted visualization experiments on flows around two-dimensional models of specific cross sections of the forewings and hindwings. For the location of the cross section, we selected the 75% semispan position,

where the profile data agreed well with those of other references (Wakeling and Ellington [2]) and the flow was likely to be two-dimensional. Wing models were made by bending an aluminum plate of 1 mm thickness. The chord length was about 20 cm, and the precision of the model construction was within 1 mm in both the streamwise and transverse directions. The veins of a real dragonfly wing have minute protuberances and spines, which are neglected here.

Mean flows and some features of vortices around the wing models are shown in Fig. 2 at an angle of attack of 5 deg and three values of Re. The flows mainly around the hindwings will be shown here. The exposure time for Fig. 2a is 0.5 s, during which the flow passes through a distance roughly equal to the vortex diameter; the exposure time for Fig. 2d is 5 s and that for Fig. 2f is 13 s. The exposure time for Figs. 2b, 2c, and 2e is about 0.02 s.

Figure 2a shows that the region of mean vortices around the hindwing model of a dragonfly of the species *Anax parthenope* takes the shape of an airfoil, around which the flow passes its periphery as if the flow were along that airfoil. We may interpret this situation as that of an "air caterpillar" which consists of an airfoil-shaped fairing belt moving in the same direction as the outer flow that covers the original wing. The train of vortices may be regarded as the driving wheels and their perimeter may constitute the outer belt passing around the wheels. It can be seen from Figs. 2a and 2b that vortices are generated successively at the leading edge of the hindwing at $Re \approx 7000$, and that, as these vortices move downstream, they are disintegrated by collisions with the following wing corrugations, forming new vortices, and eventually arrive at its trailing edge. It can also be seen that, under the wing, weak standing vortices are formed which fill the hollows, allowing the outer flow to pass almost uninterrupted. In other words, the vortex train moving along the upper surface of the dragonfly's wing facilitates the convex bending of the upper flow without loss of energy, while the weak standing vortices filling the underlying hollows of the wing facilitate the smooth downstream flow of the outer stream rather than a course along the rugged wing surface.

Figure 2c shows vortices around the forewing; the overwing vortices are regularly positioned in a train and do not disintegrate at the trailing edge at the same Re as the hindwing. Figure 2d shows the mean flow around the same wing. The generation of vortices around the hindwing when Re is reduced to 3500 is shown in Fig. 2e. The behavior of the vortices appears to be tamed and of similar appearance to the vortex train on the relatively less-rugged forewing at $Re \approx 7000$, as in Fig. 2c. When the leading-edge protuberance is less rugged, as on the forewings, the vortex behavior seems to become gentler to exhibit a regular lining up, but when the protuberance is more pronounced, as on the hindwings, a similar lining up of vortices appears at half the previous Re. As for Fig. 2e, the Reynolds number based on twice the height of the leading-edge protuberance is about 160, which corresponds to a flow velocity range where the Strouhal number for vortex shedding changes with the Reynolds number (Kovasznay [11]); in this range, the frequency of vortex generation decreases sharply.

As can be observed in Fig. 2f, despite the fact that the vortices over the upper surface of the wing are not of the vortex-train type but of the standing-vortex type when Re is decreased to 2000, the mean streamlines around the wing sustain an airfoil flow pattern; consequently, the air caterpillar still fulfills its function despite the decrease of the Strouhal number associated with the leading-edge height. The corrugated wing of the dragonfly *Anax parthenope* is thus capable of sustaining its functions as an airfoil, even when the standing-type vortices, as opposed to the vortex trains, begin to cover the wing with the sharp decrease of Strouhal number at small Re.

Using either way, gliding dragonflies seem to control the air flow by forming the small microscale "caterpillar-belt" flows; these comprise part of the fluid flow along the upper and lower wing surfaces over a relatively wide range of Re.

We further investigated how the flow over the wing evolves due to acceleration with the use of an acceleration apparatus where the back-and-forth movable support of the models is attached to a dolly, which can also be moved independently of the water tank at precisely controlled constant velocities. The results of experiments conducted using a thin cambered airfoil and a two-dimensional model of the hindwing of *Anax parthenope* are shown in Fig. 3.

As can be observed in Figs. 3a and 3b, the separated flow region on the cambered airfoil narrows in thickness after acceleration, and the outer mean streamlines increase their upward convexity to augment the lift coefficient. During the time in which the uniform flow covered about five chord lengths, the separated region resumed its pre-acceleration thickness and consequently the mean streamlines also resumed their former shapes.

This phenomenon means that the cambered airfoil increases its total lift significantly by increasing both the lift coefficient and dynamic pressure for a certain time after acceleration. If the increase in flow velocity occurs over both wings, this may lead to a gain in altitude of the airframe, whereas if it occurs on one wing only, a rolling motion may be instigated. In addition, the reduction in the thickness of the separated region results not only in an increase in the lift coefficient but also in a reduction of the drag coefficient, and this causes a reduction in resistance against various movements; such a reduction is not desirable from the viewpoint of ensuring dynamic stability.

On the other hand, as Figs. 3c and 3d show, a corrugated wing does not change the overall pattern of the mean streamlines even after acceleration, and its lift coefficient may also remain unchanged. Thus, when the corrugated wings are accelerated, they do not affect such a consequential change of aerodynamic characteristics as experienced by cambered airfoils.

In low-Re flight, a dragonfly's corrugated wing will give the flying object a superior flight stability than conventional smooth-profiled wings, such as curved plates.

Acknowledgments

This work was financed by the Ministry of Education, Science, and Culture of Japan, and Nippon Bunri University. S. Sinohara acknowledges the support of the Japan Student Services Organization.

References

[1] Okamoto, M., Yasuda, K., and Azuma, A., "Aerodynamic Characteristics of the Wings and Body of a Dragonfly," *The Journal of Experimental Biology*, Vol. 199, Feb. 1996, pp. 281–294.

[2] Wakeling, J. M., and Ellington, C. P., "Dragonfly Flight, I: Gliding Flight and Steady-State Aerodynamics," *The Journal of Experimental Biology*, Vol. 200, Feb. 1997, pp. 543–556.

[3] Kesel, A. B., "Aerodynamic Characteristics of Dragonfly Wing Sections Compared with Technical Airfoils," *The Journal of Experimental Biology*, Vol. 203, Oct. 2000, pp. 3125–3135.

[4] Sunada, S., Yasuda, T., Yasuda, K., and Kawachi, K., "Comparison of Wing Characteristics at an Ultralow Reynolds Number," *Journal of Aircraft*, Vol. 39, No. 2, March–April 2002, pp. 331–338. doi:10.2514/2.2931

[5] Azuma, A., *The Biokinetics of Flying and Swimming*, 2nd ed., AIAA Education Series, AIAA, Reston, VA, 2006, pp. 223–226.

[6] Ellington, C. P., "Insects Versus Birds: The Great Divide," AIAA Paper 2006-35, 2006.

[7] Tamai, M., Wang, Z., Rajagopalan, G., Hu, H., and He, G., "Aerodynamic Performance of a Corrugated Dragonfly Airfoil Compared with Smooth Airfoils at Low Reynolds Number," AIAA Paper 2007-0483, 2007.

[8] Karman, T. V., *Aerodynamics: Selected Topics in the Light of Their Historical Development*, Cornell Univ. Press, New York, 1954.

[9] Taneda, S., "Experimental Investigations of the Wake Behind Cylinders and Plates at Low Reynolds Numbers," *Journal of the Physical Society of Japan*, Vol. 11, No. 3, 1956, pp. 302–307. doi:10.1143/JPSJ.11.302

[10] Honji, H., "Downstream Persistence of Regular Vortex Streets," *Journal of the Physical Society of Japan*, Vol. 55, No. 8, 1986, pp. 2897–2898. doi:10.1143/JPSJ.55.2897

[11] Kovasznay, L. S. G., "Hot-Wire Investigation of the Wake Behind

Cylinders at Low Reynolds Numbers," *Proceedings of the Royal Society of London A*, Vol. 198, No. 1053, 1949, pp. 174–190.
doi:10.1098/rspa.1949.0093

F. Coton
Associate Editor